INFLUENCE OF NUCLEOTIDE STATE ON TUBULIN PROTOFILAMENTS

An Undergraduate Research Scholars Thesis

by

ERIC DAVIED

Submitted to Honors and Undergraduate Research
Texas A&M University
in partial fulfillment of the requirements for the designation as an

UNDERGRADUATE RESEARCH SCHOLAR

Approved by
Research Advisor: Dr. Wonmuk Hwang

May 2014

Major: Biomedical Engineering

TABLE OF CONTENTS

ABSTRACT

Influence of Nucleotide State on Tubulin Protofilaments. (May 2014)

Eric Davied
Department of Biomedical Engineering
Texas A&M University

Research Advisor: Dr. Wonmuk Hwang
Department of Biomedical Engineering

Microtubules are filaments within cells that play important roles in intracellular transport, cell division, and overall structural support. Microtubules are composed of tubulin dimers of α- and β-tubulin. The dimers polymerize at the (+) end of the microtubule to cause microtubule growth. β-tubulin must be bound to GTP for dimers to polymerize effectively. Microtubules will undergo catastrophic fraying and depolymerization at the (+) end when only GDP-bound tubulin is present. GTP- and GDP-bound dimers in solution seem to exist in a slightly bent state, while they must straighten to polymerize in the microtubule. While the effect of GTP on microtubule stability is clear, it is not so clear exactly how GTP influences the structural integrity of the microtubule, whether it causes conformational changes in the tubulin that prepare the tubulin for polymerization, or whether it facilitates the structural switch upon polymerization. Analysis of computer simulations of protofilaments in either the GTP- or GDP-bound state could elucidate how these nucleotide states affect the curvature of intra and inter dimer linkages and the force required for straightening. Our analysis indicated that nucleotide state did not influence the curvature or flexibility of solvated protofilaments in a way to facilitate polymerization. The GTP-bound protofilament had greater curvature by the end of simulation. Further analysis of protofilaments aligned to a microtubule image or with lateral contacts in place is recommended.

CHAPTER I

INTRODUCTION

Microtubules are filaments within cells that play important roles in intracellular transport, cell division, and structural integrity. The structure of a microtubule is a long hollow cylinder, composed of a ring of parallel filaments varying in circumference from 8 to 20 filaments in vivo[1]. Microtubules have high compressive strength, but must have some lateral flexibility so they do not break under shear. The variability in protofilament numbers to form the ring (and thus variable lateral curvature) is in line with the lateral flexibility microtubules exhibit[2]. Filaments are composed of heterodimers of α- and β-tubulin proteins linked together longitudinally. Microtubules are polarized, so that the α-tubulins of the dimers point towards the (-) end of the microtubule, and the β-tubulins point towards the (+) end. Polymerization occurs at the (+) end of the microtubule to cause microtubule growth. (The (-) end is usually anchored by capping proteins). In order to polymerize, the β-tubulin should be bound to a GTP, whereas a structural GTP is always bound to the α subunit[3]. Microtubule polymerization occurs as longitudinal contacts form in the axial direction of the filament, and adjacent tubulins interact laterally.

Over time, the β-tubulin GTP may be hydrolyzed to GDP. Since microtubules polymerize in the (+) direction, the β-tubulins near the (-) end are GDP-bound, while the (+) end tubulins form a GTP-bound stabilizing "cap". If the GTP in this cap become hydrolyzed to GDP, the (+) end becomes unstable, and strands of GDP-bound tubulin will curve outwards and fray off, causing catastrophic depolymerization of the microtubule. The microtubule may then be rescued by

binding of GTP-bound tubulin, and polymerization can occur again. This interplay between slow growth and catastrophic decay is referred to as "dynamic instability." Upon polymerization, protofilaments, short chains of longitudinally attached dimers, must straighten and connect to each other laterally to complete the microtubule cylindrical structure[2]. When protofilaments adopt the curved conformation, lateral contacts in the microtubule are broken and rapid depolymerization takes place[4]. Thus, protofilaments are the basic building blocks of microtubules and lateral connections and straightening of the dimers are key to polymerization.

In vivo, microtubule dynamics are regulated by different classes of proteins at the different ends. (-) ends are usually capped and do not grow nor shrink, whereas (+) ends are dynamic[5]. Microtubules can be stabilized by drugs such as taxol and GMPCPP to prevent depolymerization. GMPCPP is like a non-hydrolysable analog of GTP. Taxol stabilizes microtubules by causing a conformational change in tubulin favoring the straightened conformation. Stathmin favors depolymerization of microtubules by binding to and encouraging curving of protofilaments.

Currently, there are two models by which GTP may promote polymerization and GTP hydrolysis induces disassembly. The allosteric model predicts that GTP directly causes the dimer straightening necessary for polymerization. The lattice model, on the other hand, predicts that dimers of both nucleotide state are bent when free in solution, but that GTP enables the structural switch to the straight conformation upon polymerization by facilitating or strengthening lateral contacts.

It remains under debate whether this transformation is directly linked to the nucleotide state, or a

consequence of the longitudinal or lateral contacts in the MT lattice. Previous experiments lend evidence in support of both models. In support of the allosteric model, curvature of structures bound to GMPCPP, a GTP analog, were found to be smaller than that of GDP-tubulin[6]. However, it is now generally accepted that free tubulin dimers are curved for both nucleotide states[5][3]. While more evidence for the lattice model is forthcoming, the mechanism for how GTP promotes polymerization, and likewise how hydrolysis of the (+) end causes depolymerization, is still not entirely clear.

In support of the lattice model, previous atomistic simulations of single tubulin dimers have suggested intrinsic bending of the dimers for both nucleotide states[6]. In addition, X-ray crystal structures of (+) end capped GTP-tubulin suggest that GTP facilitates the tubulin structural switch that accompanies microtubule assembly but does not trigger it in unpolymerized tubulin[5]. However, these findings are limited by the previous inavailability of high-resolution crystal structures of GTP-bound tubulin.

In solution, the structures of GTP-tubulin and GDP-tubulin differ locally in the neighborhood of the nucleotide[3]. By examining structures of protofilaments bound to a stathmin-like protein, which binds to the sides of protofilaments, one study found that soluble GTP-tubulin experiences a loop movement that may facilitate the curved to straight transition upon polymerization[3]. This suggests that straightening of the dimer occurs as additional contacts form during polymerization[3]. When tubulin depolymerizes, these lateral contacts are broken, and protofilaments curve off of the microtubule while maintaining longitudinal contacts. This suggests that the strength of the lateral contacts may be the determining factor for microtubule polymerization [2]. This supports the lattice model, as the GTP may cause changes that prepares

the tubulin for straightening, but not directly causing the straightening itself. Additional simulations suggest that the GTP may induce changes in the H1-S2 loop[2] and allows more stable longitudinal bonds by causing a shift in the T3 and T5 loops and the central helix[3], which place the H1-S2 loop and M-loop in position to form stronger lateral contacts[7]. Figure 1 shows the H1-S2 loop and the M-loop of the β-tubulin highlighted in the tubulin dimer.

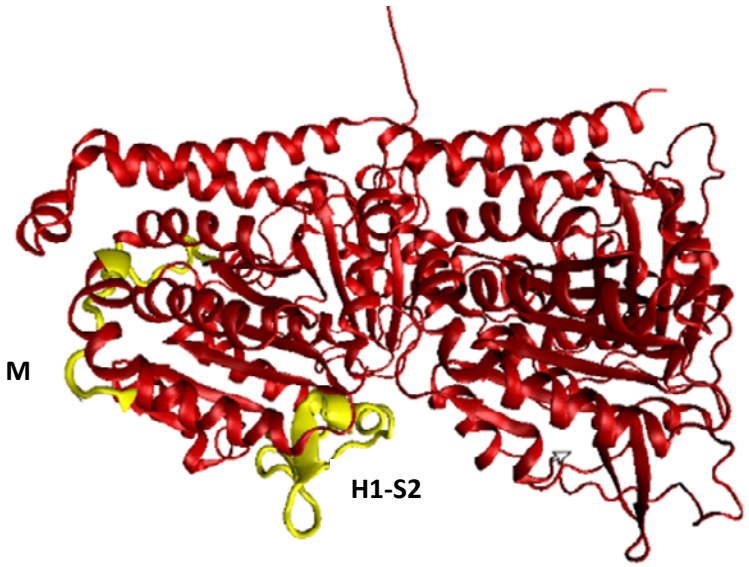

Figure 1: Tubulin dimer with H1-S2 loop and M loop of β-tubulin highlighted in yellow, from PDB entry 3RYI[3]

Analysis of high-resolution atomistic models of protofilaments in either the GTP or GDP-bound state could elucidate how these nucleotide states affect the conformation of tubulin in either the curved or straight conformation. The advantage of atomistic simulation is that it is free from the destabilizing agents or capping proteins that are usually used to isolate microtubule protofilaments, which could be influencing tubulin conformation and curvature. However, atomistic simulations are limited by the small timescales they can sample and by the number of atoms comprising the tubulins and solvent, limiting the simulation to short protofilaments. While free from external factors, simulations do rely on the accuracy of the underlying force

fields. Analysis of protofilaments free in solution could offer insight into how the nucleotide state affects the curvature of intra- and inter-dimer linkages. If GTP-bound protofilaments experience less curvature, GTP may be causing an allosteric effect that favors microtubule polymerization. In addition, if GTP-bound protofilaments have lower flexural rigidity, the force and thereby the energy barrier for straightening and polymerization would be lowered. Additional experiments such as overlaying atomistic models on EM images could provide the force required for straightening. Additionally, mechanistic analysis of tubulin sheets could provide information about the lateral contacts that may play a significant role in stabilization of the straight conformation.

CHAPTER II

METHODS

Structural data for tubulin molecules was downloaded from the Protein Data Bank (PDB). CHARMM (Chemistry at HARvard Molecular Mechanics) software was used to model and simulate tubulin structures. Visual Molecular Dynamics (VMD) was used for visualization and qualitative inspection of the models.

Simulation of GTP-bound dimer

The first simulation was conducted was that of a GTP-bound tubulin dimer free in solution (PDB ID 4DRX[5]). The dimer was built in CHARMM, and modloop was used to complete coordinates for residues that were missing from the PDB file. Its structure was compared to that of a straight tubulin dimer, the structure of which had been obtained from zinc-induced sheets stabilized with taxol (PDB ID 1JFF[8]). The bending angle was measured by aligning the α-tubulins (minus residues that were initially missing or did not match) and measuring the angle change of the vector joining the centers of mass of the α- and β-tubulins.

Next, the model was solvated and neutralized. An explicit solvent environment was built by building a cube with water molecules and ions around the dimer. The system was neutralized by addition of an appropriate amount of Mg^{2+}, Na^{+}, and Cl^{-}. Mg^{2+} was added in a concentration of 4 mM, and Na^{+} in 50 mM, to mimic the intracellular environment, and then the appropriate number of Cl^{-} for an overall neutral charge in the system. This cubic box of solvent was used to set up a cubic periodic boundary condition for the system.

Next, energy minimization was conducted. First, the water and ions that were added during solvation and neutralization were minimized. All molecules from the original crystal were fixed during this step. Minimization was conducted with 500 steps steepest descent (SD), and 500 steps adopted basis Newton-Raphson method (ABNR). Next a series of minimizations with 200 steps SD and 200 steps ABNR were conducted. Five minimizations were conducted, with decreasing harmonic force constraints. The protein backbone was restrained with k={40, 30, 20, 0, 0} kcal/mol, and other molecules from the original crystal structure were restrained with k={20, 15, 10, 5, 0} kcal/mol in each run.

Heating and equilibration were then performed. Domain decomposition was utilized for this and subsequent tasks, a method of parallelizing the simulation, dividing the simulation box into 8 x 8 x 8 sub-boxes. Heating was done from 30 K to 300 K using the Leapfrog Verlet integrator for 100 ps with a harmonic force constraint of 5 kcal/mol on the tubulin backbones and nucleotides. Equilibration was conducted using the Leapfrog Verlet integrator for 200 ps under constant pressure and temperature.

The production run of 2 ns was conducted using the Leapfrog Verlet integrator, constant pressure and temperature, and a Hoover thermostat at 300 K.

Simulation of GTP- and GDP-bound protofilaments

A protofilament of GTP-bound tubulin was constructed based on a structure of two dimers bound to a stathmin-like domain (PDB ID 3RYF[3]). The two-dimer structure was built in CHARMM, and coordinates for missing residues were filled in by alignment to the tubulin constructed earlier

from 4DRX. A 3-dimer protofilament was then constructed by copying the molecule and aligning the α-tubulin in the first dimer over the α-tubulin in the second. To illustrate, if the original structure and its copy were a1-b1-a2-b2 and a1*-b1*-a2*-b2* the new structure was a1-b1-a1*-b1*-a2*-b2* by alignment of a1* over a1, and deletion of a2 and b2. This alignment was chosen to accurately preserve inter- and intra-dimer contacts. A GDP-bound protofilament was constructed in similar fashion based on PDB ID 3RYI[3]. A protofilament is shown below in Figure 2 for reference.

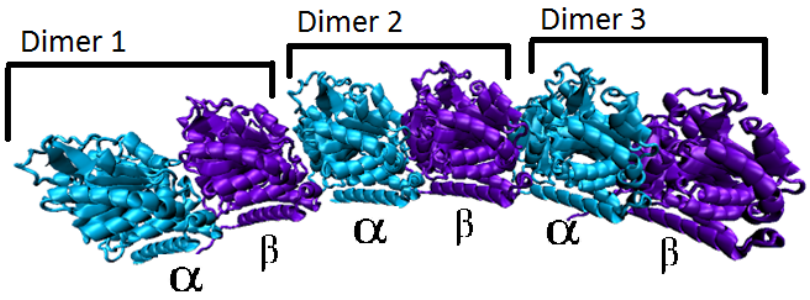

Figure 2: 3-Dimer protofilament with labelled dimers and α- and β-tubulins

Solvation, neutralization, heating, and equilibration for each protofilament were then conducted in similar fashion as done for the dimer in the earlier section. The production run of 25.2 ns was conducted using the Leapfrog Verlet integrator, constant pressure and temperature, and a Hoover thermostat at 300 K.

Construction of triads

Twist and bending angles were measured in the protofilament by construction of triads at the center of each tubulin monomer and measuring the Euler angles between consecutive triads. The two central β-sheets and the nucleotide of each tubulin monomer were used to construct triads.

The center of the triad was set at the center of mass of the two β-sheets. $\hat{e}_3$ was then set as the normalized vector from the center of the triad to the center of mass of the nucleotide. $\hat{e}_2$ was set as the normalized vector from the center of the triad to the center of mass of the first β-sheet. $\hat{e}_1$ was then found by taking the cross product of $\hat{e}_3$ and $\hat{e}_2$. A tubulin dimer with triads in place is shown in Figure 3.

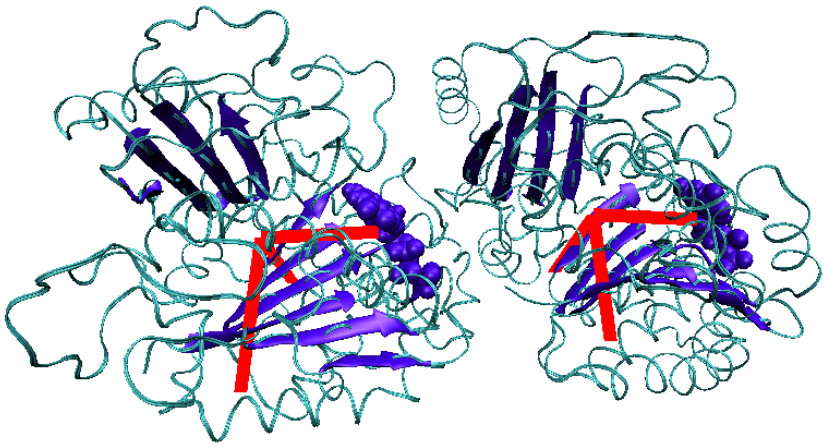

Figure 3: Tubulin dimer with triads (red). The nucleotides and β-sheets are highlighted in violet. $\hat{e}_3$ points to the right, towards the nucleotide. $\hat{e}_2$ points down, through the first β-sheet. $\hat{e}_1$ points into the page.

Measuring bending angles

We used variation in Euler rotation angles between successive triads to calculate bending stiffness.

We constructed matrices X and X' containing the vectors of consecutive triads, so X = [$\hat{e}_1$; $\hat{e}_2$; $\hat{e}_3$], and X' = [$\hat{e}_1$'; $\hat{e}_2$'; $\hat{e}_3$']. Using a Cartesian coordinate basis E = [$\hat{x}, \hat{y}, \hat{z}$], we have X=AE and X'=BE, where A and B are 3 x 3 matrices containing the Cartesian components of X and X', respectively. Thus, we can define rotation matrix R where

$$X'=RX \text{ and } R \equiv BA^{-1} \quad (1)$$

R can be broken down into three basic rotation matrices $R=R_1R_2R_3$, where

$$R_1(\theta_1) = \begin{pmatrix} 1 & 0 & 0 \\ 0 & \cos\theta_1 & -\sin\theta_1 \\ 0 & \sin\theta_1 & \cos\theta_1 \end{pmatrix}, R_2(\theta_2) = \begin{pmatrix} \cos\theta_2 & 0 & \sin\theta_2 \\ 0 & 1 & 0 \\ -\sin\theta_2 & 0 & \cos\theta_2 \end{pmatrix}, \text{ and}$$

$$R_3(\theta_3) = \begin{pmatrix} \cos\theta_3 & -\sin\theta_3 & 0 \\ \sin\theta_3 & \cos\theta_3 & 0 \\ 0 & 0 & 1 \end{pmatrix}$$

$\theta_1, \theta_2,$ and θ_3 represent roll, pitch, and yaw, respectively, as used in flight dynamics terminology. For our purposes θ_1 represents twisting, and θ_2 and θ_3 represent bending of the microtubule. Since A and B are known, these angles can be solved for by solving Equation (1) for R, and using $R=R_1R_2R_3$,

$$R = \begin{pmatrix} \cos\theta_2 \cos\theta_3 & -\cos\theta_2 \sin\theta_3 & \sin\theta_2 \\ \cos\theta_1 \sin\theta_3 + \sin\theta_1 \sin\theta_2 \cos\theta_3 & \cos\theta_1 \cos\theta_3 - \sin\theta_1 \sin\theta_2 \sin\theta_3 & -\sin\theta_1 \cos\theta_2 \\ \sin\theta_1 \sin\theta_3 - \cos\theta_1 \sin\theta_2 \cos\theta_3 & \sin\theta_1 \cos\theta_3 + \cos\theta_1 \sin\theta_2 \sin\theta_3 & \cos\theta_1 \cos\theta_2 \end{pmatrix}$$

θ_1=atan2(-R(2,3),R(3,3)), θ_2=arcsin(R(1,3)), and θ_3=atan2(-R(1,2),R(1,1)), where R(row,column) is the element of R at that row and column. atan2(y,x) is a variation of the arctangent function; it returns the angle between the positive x-axis of a plane and the point (x,y). The angle is positive for y>0 (counter-clockwise angles), and negative for y<0 (clockwise angles). Since there are 6 triads, and we are measure the angle between consecutive triads, we obtain bending information at 5 points.

Measuring bending stiffness

Total elastic bending energy on a bending angle θ for n triads in a rod whose equilibrium shape is straight can be expressed as

$$\frac{1}{2}\sum_{i=1}^{n} k_i\theta_i^2 \qquad (2)$$

where θ_i is the bending angle and k_i is the bending rigidity of triad i[9]. The elastic energy between two consecutive triads with separation distance Δs is then

$$E(s)=\frac{1}{2}\sum_{i=1}^{3} k_i\omega_i^2 \quad (3)$$

where ω_i is the bending rate of a triad with respect to distance, $\theta_i/\Delta s$, for each Euler bending angle. For a rod that is not straight, Equation (3) can be generalized as

$$E(s)=\frac{1}{2}\sum_{i=1}^{3} k_i(\omega_i-\omega_{i0})^2 \quad (4)$$

where ω_{i0} is the equilibrium curvature[10]. Since the protofilament is at thermal equilibrium at temperature T, the average elastic energy stored between two consecutive triads with separation distance Δs satisfies the equipartition theorem

$$\langle E(s)\rangle \Delta s = \frac{k_B T}{2} = \frac{k_i}{2}\langle(\omega_i-\omega_{i0})^2\rangle \Delta s \quad (4)$$

where $\langle\cdot\rangle$ denotes time average, k_B is Boltzmann's constant, and k_i is bending stiffness.

We used Euler angles θ_2 and θ_3 to calculate k for each triad. We plotted the values of these angles on a two-dimensional scatterplot with axes θ_2 and θ_3, and found the line of best fit. We centered and rotated this graph so that the new x-axis was along the line of best fit. For the variance $\langle(\omega-\omega_0)^2\rangle$, in Equation (4), we used the x and y coordinates of the rotated points to find bending energy in the principal axis of bending and the axis perpendicular to it. We solved for k in these directions for each triad, and in the θ_2 and θ_3 directions.

$d\vec{z}$ projections

We also used the change of the $\hat{e}_3$ vector between two triads to quantify flexibility. Considering two consecutive triads, where the second is denoted by ', $d\vec{z} = \hat{e}_3' - \hat{e}_3$. $d\vec{z}$ was projected onto $\hat{e}_1$ and $\hat{e}_2$. These values were plotted as points on a two-dimensional scatterplot for each triad, manifesting as an oval of points. The oval was centered at the origin, and the line of best fit was found[9]. This line represents the principal axis of bending in the $\hat{e}_1$ $\hat{e}_2$ plane. Standard

deviation of the projections along this axis and the axis perpendicular to it were measured as a quantification of flexibility. Standard deviations were also calculated along the $\hat{e}_1$ and $\hat{e}_2$ dimension.

CHAPTER III

RESULTS

Bending angles

The twist (θ_1) and bending (θ_2 and θ_3) angles within the three dimers of the GDP-bound and GTP bound protofilaments are shown below in Figure 4.

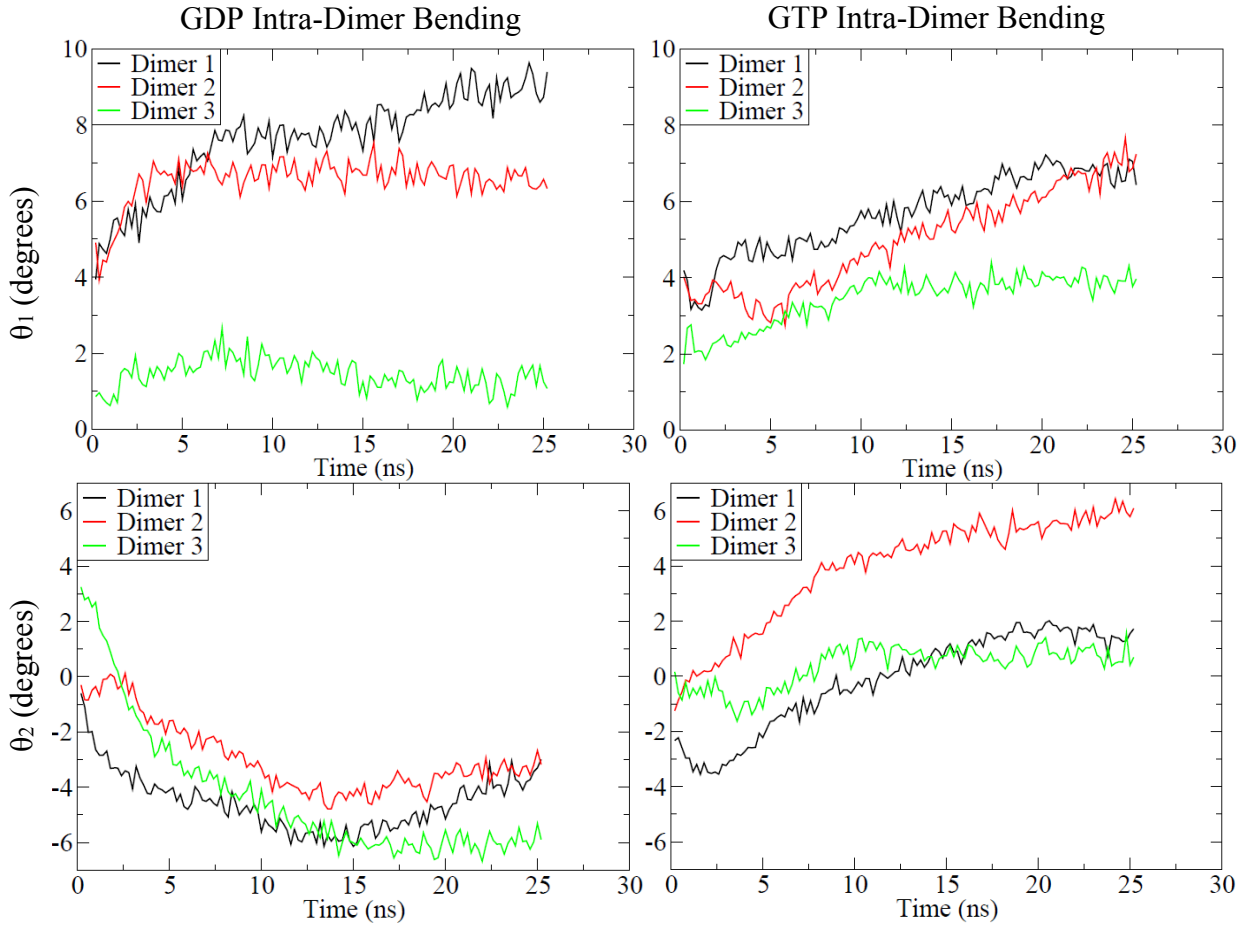

Figure 4: Intradimer twist and bending angles of within dimers.

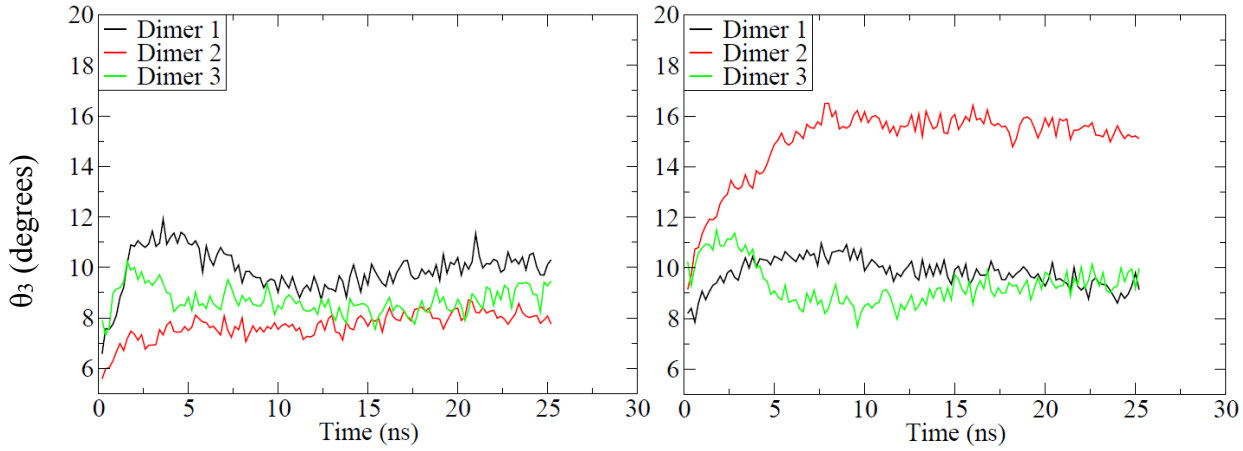

Figure 4: Continued.

There was no general trend in one type of protofilament having consistently higher bending than the other. The protofilaments bent in opposite directions regarding θ_2, and bending was relatively small in this direction for most dimers. The largest difference occurred in θ_3 with most bending in dimer 2 of the GTP protofilament, with other dimers experiencing 8-10° of bending in this direction. The twist and bending angles between dimers is shown below in Figure 5.

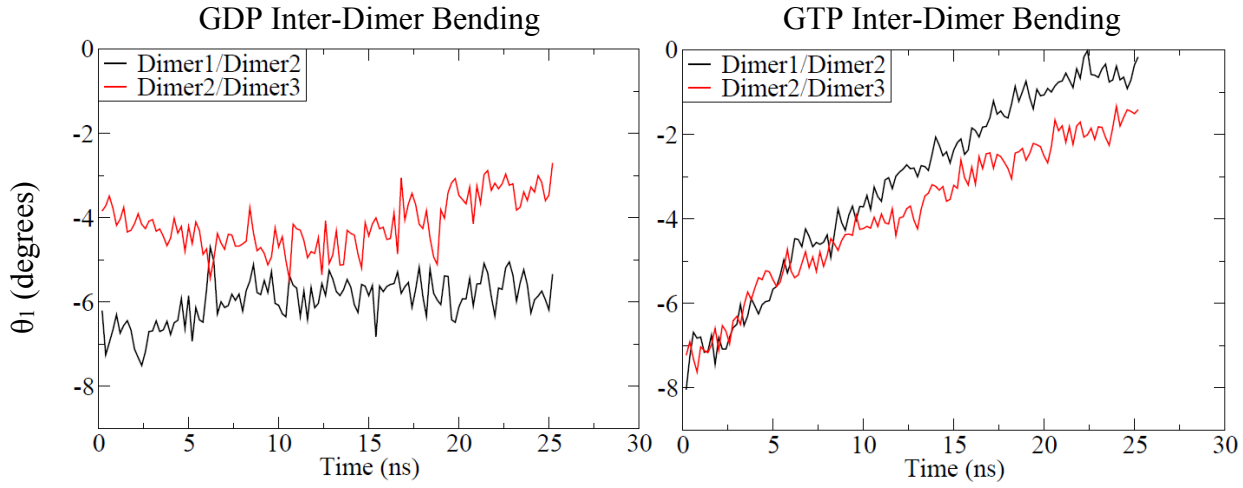

Figure 5: Intradimer twist and bending angles of within dimers.

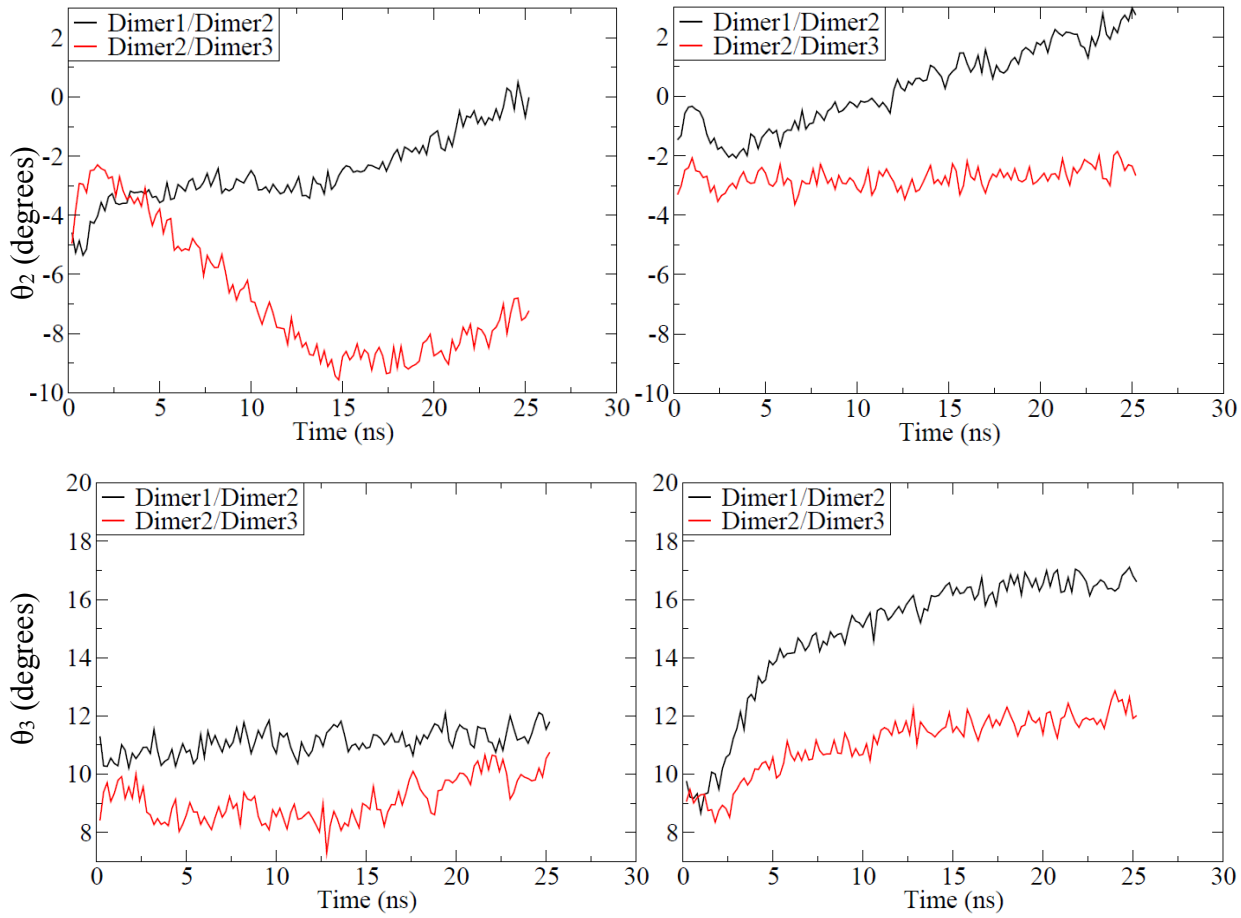

Figure 6: Continued.

Figure 5 shows a greater degree of bending between dimers 2 and 3 in the θ_2 direction of the GDP-bound protofilament than in the GTP-bound protofilament. However, the GTP-bound dimer showed a significantly greater degree of bending between dimers 1 and 2 in the θ_3 direction than the GDP-bound dimer did.

A screenshot (Figure 6) showing the final state of both protofilaments shows that the GTP-bound protofilament experienced a greater overall curvature than the GDP-bound protofilament.

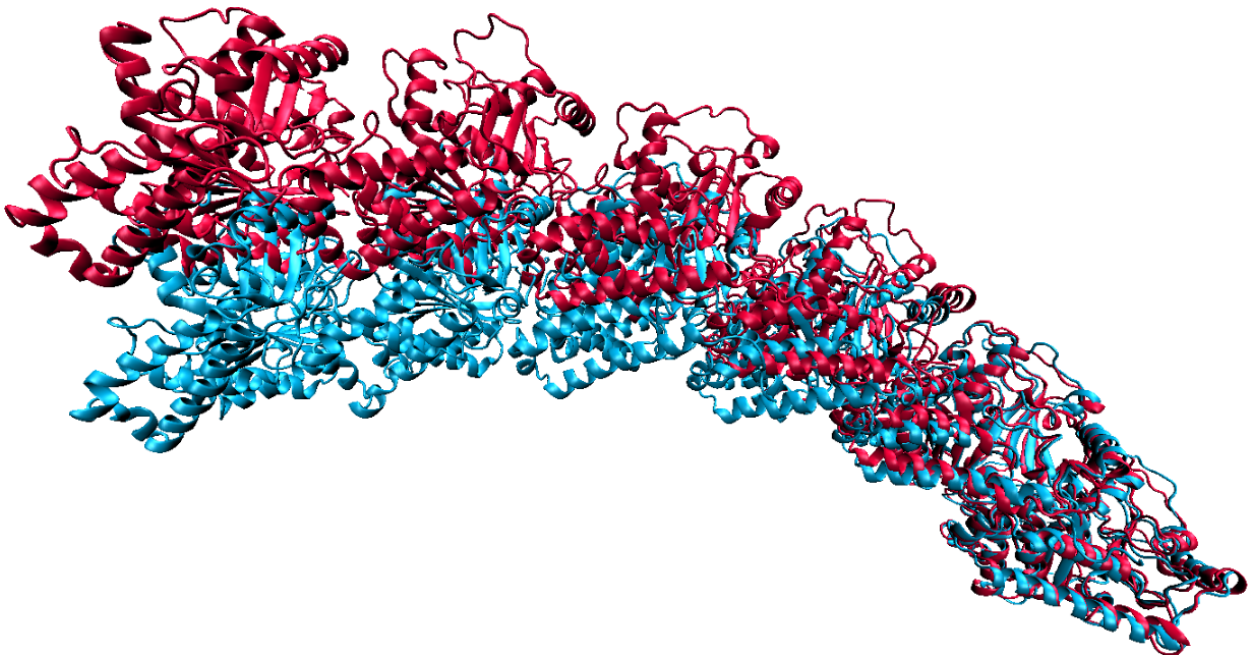

Figure 6: Final state of GDP-bound (red) and GTP-bound (blue) protofilaments after 25.2 ns simulation in explicit water and ions solvent.

Bending stiffness

The bending stiffness in the θ_2 direction (k_2), θ_3 direction (k_3), and the principal axis of bending and the axis perpendicular to it are shown in Figure 7 below. Because it took some time for bending angles to equilibrate to a stable value (see previous section), all further stiffness calculations were done using data from 17 ns – 25.2 ns.

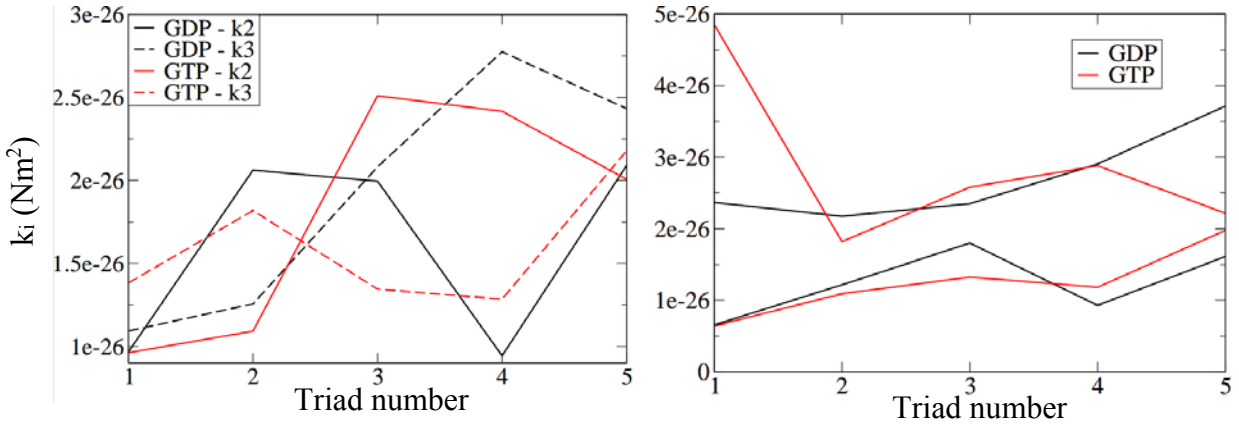

Figure 7: Bending stiffness of GDP and GTP protofilaments. The graph on the left shows stiffness in the θ_2 and θ_3 directions. The graph on the right shows stiffness in the principal axis of bending and the axis perpendicular to it.

Overall, the stiffness of the two protofilaments is similar. The spring constants in the θ_2 and θ_3 directions all fell within a similar range along the protofilament, with some variation along the triad regarding which direction expressed higher stiffness. The second graph shows even more closely matching results between the two protofilaments, except for in the principal axis of triads 1 and 5 of the GTP-bound protofilament. The stiffness is fairly low in both directions, and order of 10^{-3} less than for whole microtubules[12].

$d\vec{z}$ projections

The $d\vec{z}$ projections in the $\hat{e}_1$ $\hat{e}_2$ plane are shown in Figure 8 below for triads 1-5 (top to bottom). The orientation of the principal axes are also indicated by a solid line.

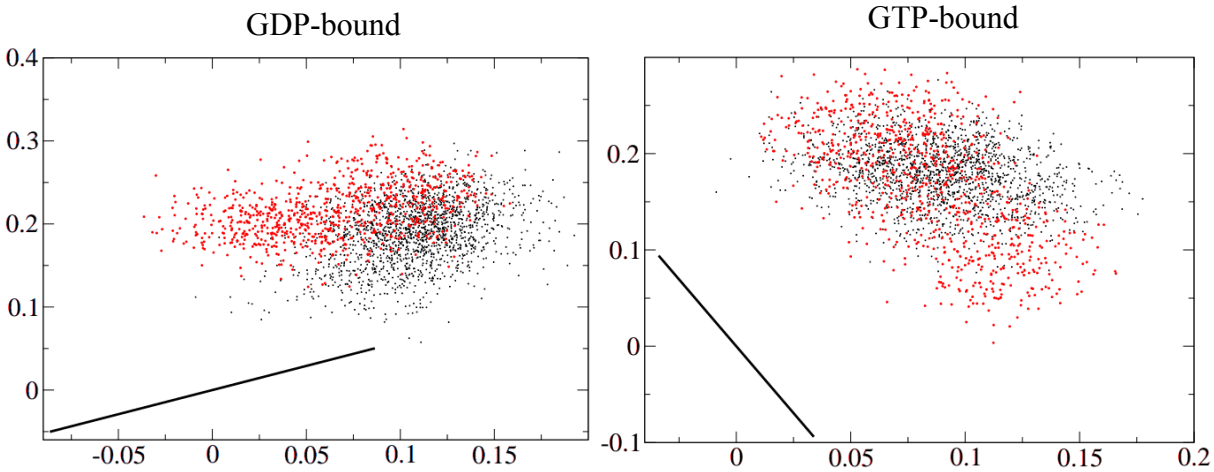

Figure 8: $d\vec{z}$ projections and principal axes of bending in the $\hat{e}_1$ $\hat{e}_2$ plane. $\hat{e}_2$ is the horizontal axis and $\hat{e}_1$ is the vertical axis. Last 820 data points are highlighted in red. Axes may not be to scale.

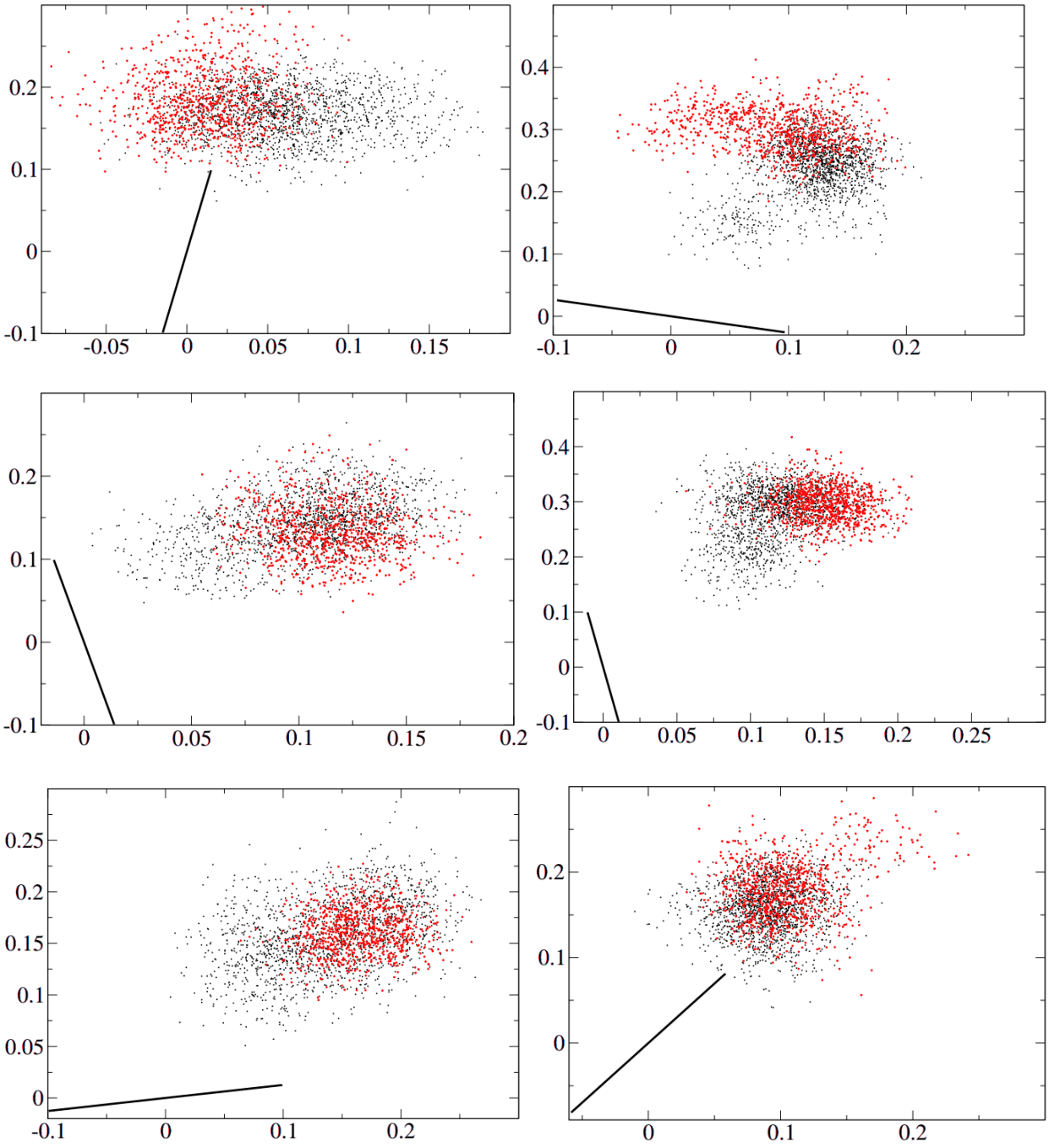

Figure 8: Continued.

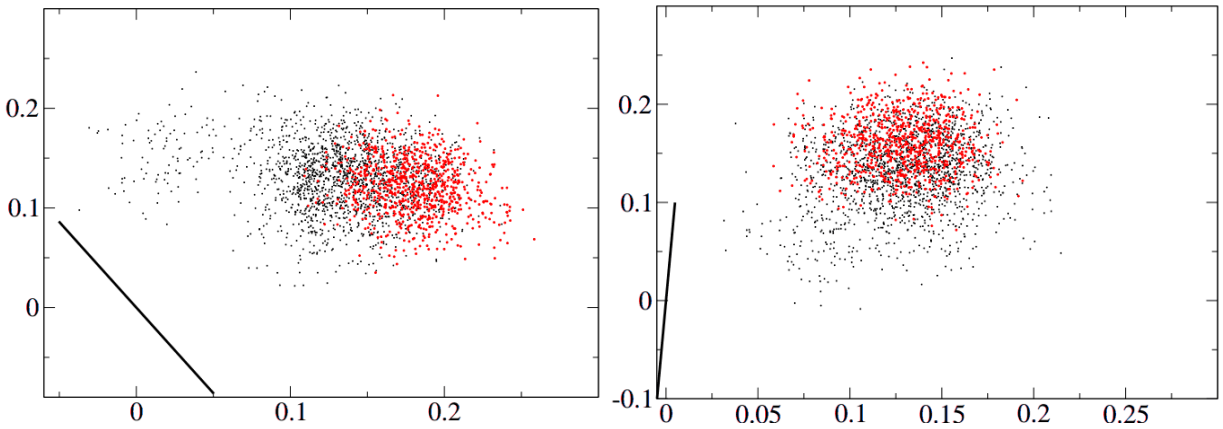

Figure 8: Continued.

Figure 8 showed variation in the direction of greatest flexibility between triads, with variation in the direction of the principal axis. As we saw in the previous part, however, the stiffness of the protofilament is not that great, and differences in flexibility for the two directions are variable along the protofilament, so that one direction is not overall more flexible than the other (left graph of Figure 7). Thus the direction of the principal axis of bending in the protofilament does not bear much significance. The standard deviation of $d\vec{z}$ projected onto the $\hat{e}_1$ and $\hat{e}_2$ axes, and the principal axis of bending and the axis perpendicular to it are shown in Figure 9 below.

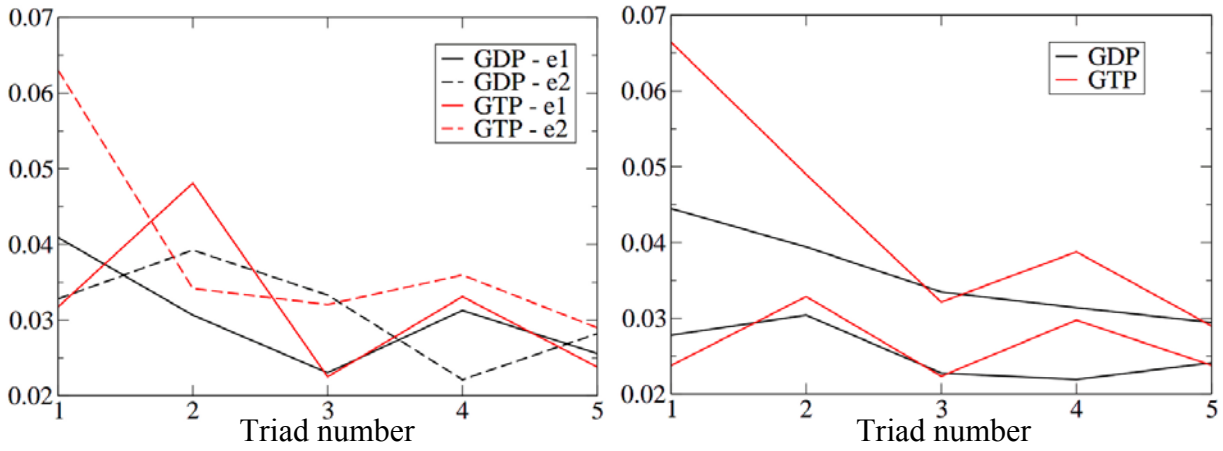

Figure 9: Standard deviation of $d\vec{z}$ projected onto the $\hat{e}_1$ and $\hat{e}_2$ axes (left graph), and the principal axis of bending and the axis perpendicular to it (right graph).

This measure of flexibility had similar results to the quantification using Euler bending angles. Neither GTP-bound nor GDP-bound protofilaments had significantly greater flexibility in one direction over the other. Most flexibilities fell within a certain range, with some variation along the protofilament as to whether GTP-bound or GDP-bound were more flexible.

Conclusion

Our analysis indicated that nucleotide state did not did not differentiate the flexibility between solvated GDP- and GTP-bound protofilaments. Analysis of bending revealed visibly greater curvature in the GTP-bound protofilament. Neither of these results indicate that GTP is involved in an allosteric effect that prepares protofilaments for polymerization, nor do they indicate that GDP causes a naturally curved state favoring depolymerization. Further analysis of protofilaments aligned to the microtubule structure or with lateral contacts in place is recommended. For the former, force required for straightening could be measured for both nucleotide states. For the latter, observation of lateral contacts and lateral binding forces could be observed. Because lateral contacts are formed and broken during polymerization and depolymerization, such an analysis may be especially critical to elucidate the role GTP may play in the lattice model of polymerization explained in the introduction of this report. While this report observed bulk mechanical properties of the protofilaments, a more detailed look at movement of domains such as the T3, T5, H1-S2, and M loop could also be conducted.

REFERENCES

[1] K.J. Bohm, W. Vater, H. Fenske, E. Unger. Effect of microtubule-associated proteins on the protofilament number of microtubules assembled in vitro. *Biochim. Biophys. Acta*, 800:119-126, 1984.

[2] Haizin Sui, Kenneth H. Downing. Structural basis of interprotofilament interaction and lateral deformation of microtubules. *Structure*, 18:1022-1031, 2010.

[3] Agata Nawrotek, Marcel Knossow, Benoit Gigant. The determinants that govern microtubule assembly form the atomic structure of GTP-tubulin. *J. Mol. Bio.*, 412:35-42, 2011.

[4] Ralmond B.G. Ravelli, Benoit Gigant, Patrick A. Curmi, Isabelle Jourdain, Sylvie Lachkar, Andre Sobel, Marcel Knossow. Insight into tubulin regulation from a complex with colchicine and a stathmin-like domain. *Nature*, 428:198-202, 2004.

[5] Ludovic Pecquer, Christian, Duellberg, Birgit Dreier, Qiyang Jiang, Chunguang Wang, Andreas Pluckthun, Thomas Surrey, Benoit Gigant, and Marcel Knossow. A designed ankyrin repeat proein selected to bind to tubulin caps the microtubule plus end. *PNAS*, 109(30):12011-12016, 2012.

[6] Andrea Grafmuller, Gregory A. Voth. Intrinsic bending of microtubule protofilaments. *Structure*, 19:409-417, 2011.

[7] Andrea Grafmuller, Eva G. Noya, Gregory A. Voth. Nucleotide-dependent lateral and longitudinal interactions in microtubules. *J. Mol. Biol.*, 425:2232-2246, 2013.

[8] J. Lowe, H. Li, K. H. Downing, E. Nogales. Refined structure of α-β-tubulin at 3.5 A Resolution. *J. Mol. Biol.*, 313:1045-1057, 2001.

[9] Stephanie Geggier and Alexander Vologodskii. Sequence dependence of DNA bending rigidity. *PNAS*, 107(35):15421–15426, 2010.

[10] Casa Software Ltd. Matrices and statistics. http://www.casaxps.com/help manual/mathematics/top-page.htm, 2012.

[11] Sirsish Kaushik Lakkaraju and Wonmuk Hwang. Modulation of elastic-ity in functionally distinct domain of the tropomyosin coiled-coil. *Cell. Mol. Bioeng*, 2(1):57–65, 2009.

[12] Frederick Gittes, Brian Mickey, Jilda Nettleton, and Jonathon Howard. Flexural rigidity of microtubules and actin filaments measured from thermal fluctuations in shape. *JCB*, 120:923-934, 1993.